

G. Krstulovic · M. Cencini · J. Bec

# Effective rates in dilute reaction-advection systems

May 10, 2022

**Abstract** A dilute system of reacting particles transported by fluid flows is considered. The particles react as  $A + A \rightarrow \emptyset$  with a given rate when they are within a finite radius of interaction. The system is described in terms of the joint  $n$ -point number spatial density that it is shown to obey a hierarchy of transport equations. An analytic solution is obtained in either the dilute or the long-time limit by using a Lagrangian approach where statistical averages are performed along non-reacting trajectories. In this limit, it is shown that the moments of the number of particles have an exponential decay rather than the algebraic prediction of standard mean-field approaches. The effective reaction rate is then related to Lagrangian pair statistics by a large-deviation principle. A phenomenological model is introduced to study the qualitative behavior of the effective rate as a function of the interaction length, the degree of chaoticity of the dynamics and the compressibility of the carrier flow. Numerical simulations in a smooth, compressible, random delta-correlated-in-time Gaussian velocity field support the proposed heuristic approach.

**Keywords** Chemical reactions; dilute media; transport; large deviations; Kraichnan ensemble

## 1 Introduction

Many natural and industrial processes involve the reaction or collision of diffusing species transported by an outer flow. Such systems are typically modeled in terms of the *reaction-diffusion-advection* equation for the density field  $\rho$ . In the simple case of the pair-annihilation reaction  $A + A \rightarrow \emptyset$ , where two molecules react together to become inert, this kinetic equation takes the form

$$\partial_t \rho + \nabla \cdot (\rho \mathbf{v}) = -\Gamma \rho^2 + \kappa \nabla^2 \rho, \quad (1.1)$$

where  $\kappa$  is the diffusion constant,  $\mathbf{v}$  the velocity of the outer flow, and  $\Gamma$  the reaction rate. An important aspect withheld in such an approach is the assumed relation

---

Giorgio Krstulovic · Jérémie Bec  
Laboratoire Lagrange, UMR7293, Université de Nice Sophia-Antipolis, CNRS, Observatoire de la Côte d’Azur, BP 4229, 06304 Nice Cedex 4, France

Massimo Cencini  
CNR, Istituto dei Sistemi Complessi, Via dei Taurini 19, Roma, Italy

between the microscopic stochastic rate, that is the probability that two given individual molecules react, and the mesoscopic reaction propensity, that is the number of reactions per unit time and volume written here as  $\Gamma \rho^2$ . To derive (1.1) one must assume two properties to be satisfied at the coarse-graining scale from which the hydrodynamic limit is taken [30]. First, volumes at the coarse-graining scale have to contain sufficiently many particles, in order to safely disregard finite-number fluctuations. Second, each particle within this volume must have an equal probability to react with all the others — *well-mixing* hypothesis. For this second condition to be satisfied, the coarse-graining scale has to be sufficiently small, i.e. smaller than the interaction distance between particle pairs.

It is clear that in situations where the reactants are very dilute, the two conditions underlying (1.1) might not be simultaneously satisfied. In particular, fluctuations due to a finite number of reactants might be so important to invalidate the mean-field assumptions leading to (1.1). Much work has been devoted to model and study such fluctuations in situations where transport is negligible and diffusion dominates. It was shown that finite-number effects can be taken into account by adding an imaginary noise in the reaction-diffusion equation. The time evolution of statistical quantities is then obtained by averaging with respect to this noise (see [21,28] for reviews). Two equivalent approaches were independently developed using either the Poisson representation [14] or a field-theoretical description [9,24]. In both cases, it is assumed that a reaction takes place with a given rate when two particles are on the same node of a lattice. Diffusion is then modeled by a random walk. After that, the hydrodynamic limit is obtained by performing the limit of vanishing lattice spacing. Such approaches, which were developed for diffusion-limited reactions, cannot be straightforwardly extended to cases where transport cannot be neglected.

In many natural situations, the dynamics of very dilute reacting species is dominated by (possibly compressible) advection and their diffusion is almost negligible. This is the case, e.g., of dust grains growing by accretion to form planets in the early solar system [19] or of phytoplankton confined in a two-dimensional ocean layers [25]. Also, motile microorganisms in aquatic environments can detach from the fluid trajectories thanks to swimming and behave as tracers in a weakly-compressible flow [29]. Because of the large sizes of the transported species, molecular diffusion is negligible in all aforementioned examples. Another instance concerns the initiation of rain in warm clouds. Droplets, which are typically occupying a volume fraction of the order of  $10^{-6}$ , grow by coalescence to form raindrops. Because of their finite size and mass, such droplets have inertia and their dynamics decouples from the flow. When they are sufficiently small, droplets behave as tracers in an effective compressible flow that depends on the local turbulence of the carrier airflow [22]. This leads to strong and violent fluctuations both in their local spatial concentration [27] and in the rate at which they collide [11]. Classical approaches consist in using the (mean-field) Smoluchowski coagulation equation, which is a generalization of the kinetic equation (1.1) to the case of a full population with a size distribution [26]. Many questions remain open on the statistical effects of turbulence on the timescales at which rain is formed [8]. In addition very little is known on the finite-number fluctuations induced by diluteness that might also play an important role in assessing the average growth rate of droplets. The aim of this work is to develop a general framework which

can be used to address such issues. For that, we neglect diffusion and focus on particles transported by generic compressible flows. Also, we focus on the annihilation reaction  $A + A \rightarrow \emptyset$  because we expect that this simple model will capture the essence of finite-number effects in advection-reaction systems.

It is clear that, at long times, the particle number density decreases, so that this long-term asymptotics is very likely affected by finite-number effects. Kinetic approaches using (1.1) predict that, ultimately, the average number of particles decays algebraically as  $t^{-1}$  [5]. This behavior, which occurs at times much longer than the fluid velocity correlation time, can be explained in terms of an effective eddy diffusion. The flow compressibility might decrease the effective diffusivity [31], but the latter remains anyway positive [17]. Hence, at long times, the spatial fluctuations of the concentration are smoothed out and a closed equation can be written for the spatial average of  $\rho$ . Here, we find that finite-number effects enhance the long-time decay of the average number of particles. For that we consider discrete particles that are tracers of the compressible fluid flow and that annihilate with a rate  $\mu$  when they are separated by less than an interaction distance  $a$ . We show that the average number of particles does not decrease algebraically but rather exponentially as  $\exp(-\gamma t)$ . This law pertains to the statistics of the relative motion between two reactants and the exponential decay rate  $\gamma$  depends on both the microscopic rate  $\mu$  and the flow statistical properties in a non-trivial manner. The main result of this work is the introduction of a novel Lagrangian approach in terms of non-reacting particle trajectories. We exploit these ideas to express  $\gamma$  using a large-deviation principle for the time that two tracers spend at a distance below the radius of interaction  $a$ .

The paper is organized as follows. Section 2 contains basic definitions and set the general framework of this work. The  $n$ -point number-density field is introduced and is shown to obey a hierarchy of transport equations. When integrated over space, these fields correspond to the factorial moments of the number of particles that are present in the system. We then briefly discuss the zero-dimensional case and its relationship with standard studies of finite-number effects in well-mixed settings. In section 3, the hierarchy for the  $n$ -point number-density is solved by using a Lagrangian approach that consists in following the flow characteristics. At long times the particle number moments are shown to decay exponentially with a rate  $\gamma$  that does not depend on their order. An analytic expression for  $\gamma$  is given in terms of the Lagrangian statistics of (non-reacting) tracer trajectories. In section 4 we focus on the case of two particles. The exponential decay rate is then related to the time spent by the pair at a distance less than the interaction radius and is expressed in terms of the large fluctuations of the latter. Asymptotic arguments are then developed to relate the decay rate  $\gamma$  to the *microscopic* rate  $\mu$ . Section 5 contains an application to very dilute suspensions in smooth compressible Gaussian delta-correlated-in-time flows (belonging to the so-called *Kraichnan ensemble*; see, e.g., [12]). Finally, section 6 presents some concluding remarks and open questions.

## 2 Master equations in the presence of advection

### 2.1 Settings

We consider a set of particles  $\{A_i\}_{1 \leq i \leq N(t)}$  whose positions  $\mathbf{X}_i$  obey the equations

$$\frac{d\mathbf{X}_i}{dt} = \mathbf{v}(\mathbf{X}_i, t), \quad (2.1)$$

where  $\mathbf{v}$  is a prescribed  $d$ -dimensional differentiable velocity field with given isotropic, stationary, and homogeneous statistics. The velocity field  $\mathbf{v}$  is assumed to have a finite correlation time and might be compressible with *compressibility*

$$\wp = \frac{\overline{(\nabla \cdot \mathbf{v})^2}}{\text{tr}(\nabla \mathbf{v}^T \nabla \mathbf{v})}, \quad (2.2)$$

where the over line designates the average with respect to the velocity field realizations, and  $\wp \in [0 : 1]$ . The extremal values  $\wp = 0$  and  $\wp = 1$  correspond to incompressible and purely potential velocity fields, respectively. Whenever  $\wp > 0$ , the dynamical system defined by (2.1) is dissipative. Also, to maintain sufficiently generic settings, the dynamics is assumed ergodic and chaotic. Typically, when the flow is defined on a compact set, the trajectories generated by (2.1) will concentrate on a dynamically evolving strange attractor, while in the incompressible limit they remain uniformly distributed (see, e.g., [12] for more details on particle transport in compressible and incompressible flows). For the sake of simplicity, in this paper we will focus on the dynamics of tracers given by (2.1). However, the results can be straightforwardly extended to a general dynamics given by the Newton equation  $\ddot{\mathbf{X}} = \mathbf{F}(\mathbf{X}, \dot{\mathbf{X}}, t)$  as that ruling, for instance, the evolution of inertial particles [22].

The dynamics (2.1) is supplemented by binary reactions between the particles. When  $|\mathbf{X}_i - \mathbf{X}_j| < a$  the particles labeled  $i$  and  $j$  might react and annihilate (or become inert). This happens with a rate  $\mu$ . As a consequence, the number of particles  $N(t)$  in the domain will decrease from its initial value  $N(0) = N_0$  in the course of time. We suppose that the radius of interaction  $a$  is smaller than the scale at which  $\mathbf{v}$  varies. For example, in turbulent flows, this corresponds to assuming that  $a$  is smaller than the Kolmogorov length scale  $\ell_K$ . Moreover, in writing (2.1) we have neglected particle diffusion. This is justified whenever the interaction distance  $a$  is larger than the Batchelor length scale  $\ell_B = \ell_K / \sqrt{Sc}$ , where  $Sc = \nu / \kappa$  designates the Schmidt number — that is the ratio between the fluid kinematic viscosity  $\nu$  and the particle diffusivity  $\kappa$ . For applications, our settings thus reduce to very large values of the Schmidt number. We notice that the Schmidt number can be of the order of thousands or higher in organic mixtures, biological fluids and generically for particulate matter. Estimates based on Stokes–Einstein relation lead for a micro-meter sized spherical particle  $Sc \approx 1000$  in air and  $10^6$  in water.

Before discussing the master equations which describe the system, it is worth underlining that our settings involve different sources of stochasticity. First, the dynamics (2.1) has to be supplemented by initial conditions on particle positions that we choose randomly. A second source of randomness comes from the intrinsic stochasticity of the reaction process. Finally, the fluid flow is stochastic with

prescribed statistics. Consequently, ensemble averages corresponding to these different sources of randomness must be considered; the corresponding notations will be introduced when needed.

## 2.2 Master equations for $n$ -point number densities

To fully describe all interactions between the particles in the considered system, all relative positions are simultaneously needed. It is then natural to define for  $1 \leq n \leq N_0$  ( $N_0 = N(0)$  being the initial number of particles) the joint  $n$ -point number density

$$\mathcal{F}_n(\mathbf{x}_1, \dots, \mathbf{x}_n, t) = \left\langle \sum_{i_1 \neq \dots \neq i_n} \delta(\mathbf{X}_{i_1}(t) - \mathbf{x}_1) \cdots \delta(\mathbf{X}_{i_n}(t) - \mathbf{x}_n) \right\rangle_{\mu}, \quad (2.3)$$

where the brackets  $\langle \cdot \rangle_{\mu}$  stands for the ensemble average with respect to reactions only and, by convention, the sum in (2.3) is zero when  $N(t) < n$ . The particle indices  $i_k$  vary between 1 and the number  $N(t)$  of particles in each realization of the reactions. The sum is not ordered so that, by construction, the spatial averages of the  $\mathcal{F}_n$ 's are the factorial moments of the total number of particles, namely

$$F_1(t) = \int \mathcal{F}_1(\mathbf{x}_1, t) d^d x_1 = \langle N(t) \rangle_{\mu}, \quad (2.4)$$

$$F_2(t) = \iint \mathcal{F}_2(\mathbf{x}_1, \mathbf{x}_2, t) d^d x_1 d^d x_2 = \langle N(t)(N(t) - 1) \rangle_{\mu} \quad (2.5)$$

$$F_n(t) = \int \cdots \int \mathcal{F}_n(\mathbf{x}_1, \dots, \mathbf{x}_n, t) d^d x_1 \cdots d^d x_n = \left\langle \frac{N(t)!}{(N(t) - n)!} \right\rangle_{\mu}. \quad (2.6)$$

Hence,  $\mathcal{F}_n(t)/n!$  is the average number of  $n$ -uplets among the  $N(t)$  particles still present at time  $t$ .

Taking into account the transport by the flow  $\mathbf{v}$  and the reactions, the joint  $n$ -point densities (2.3) satisfy the following hierarchy of equations

$$\begin{aligned} \frac{\partial \mathcal{F}_n}{\partial t} + \sum_{i=1}^n \nabla_{\mathbf{x}_i} \cdot [\mathbf{v}(\mathbf{x}_i, t) \mathcal{F}_n] &= -\mu \mathcal{F}_n \sum_{i < j} \theta(a - |\mathbf{x}_i - \mathbf{x}_j|) \\ &\quad - \mu \sum_{i=1}^n \int \theta(a - |\mathbf{x}_i - \mathbf{x}_{n+1}|) \mathcal{F}_{n+1} d^d x_{n+1}, \end{aligned} \quad (2.7)$$

where  $\nabla_{\mathbf{x}_i} \cdot$  is the  $d$ -dimensional divergence with respect to the spatial variable  $\mathbf{x}_i$  and  $\theta$  the Heaviside function. The transport term comes from the identity

$$\frac{d}{dt} \delta(\mathbf{X}_{i_k}(t) - \mathbf{x}_k) = -\nabla_{\mathbf{x}_k} \cdot [\delta(\mathbf{X}_{i_k}(t) - \mathbf{x}_k) \mathbf{v}(\mathbf{x}_k, t)]. \quad (2.8)$$

The two terms in the right-hand side are sinks accounting for the reactions: the first includes all binary reactions between any close-enough pair among the  $n$  considered particles; the second counts the reactions of any of these  $n$  particles with another one at a distance smaller than  $a$ .

The hierarchy (2.7) for the  $n$ -point joint number density is exact and contains all information about the dynamics and statistics of the system. Moreover, it is closed at the order  $n = N_0$  and can be integrated by the method of characteristics (see Sect. 3). In the next subsection we relate this description in terms of factorial moments to standard descriptions used in the statistical physics of well-mixed chemical reactions.

### 2.3 The zero-dimensional case

When the hypothesis of *well-mixedness* is satisfied, as when for instance the interaction radius is larger than the system size, transport does not play any role in the temporal evolution of the factorial moments  $\mathcal{F}_n$  (2.3). In this zero-dimensional limit, the hierarchy of transport equations (2.7) becomes a simpler hierarchy of ordinary differential equations, i.e.

$$\frac{dF_n}{dt} = -\frac{\mu}{2} n(n-1) F_n - \mu n F_{n+1}, \quad (2.9)$$

which can be also derived from the standard master equation describing the reaction  $A + A \rightarrow \emptyset$ . Denoting with  $\mathcal{P}_N(t)$  the probability of having  $N$  particles at time  $t$ , we have [30]

$$\frac{d\mathcal{P}_N}{dt} = \frac{\mu}{2} (N+2)(N+1) \mathcal{P}_{N+2} - \frac{\mu}{2} N(N-1) \mathcal{P}_N. \quad (2.10)$$

By definition, the factorial moments are expressed in terms of  $\mathcal{P}_N(t)$  as

$$F_n(t) = \sum_{N=0}^{\infty} \frac{N!}{(N-n)!} \mathcal{P}_N(t). \quad (2.11)$$

Taking the time derivative of  $F_n(t)$  and using (2.10) yields to (2.9).

Equation (2.10) is generally the starting point for describing the statistics of chemical reactions. In the limit of large number of particles, the mean-field approximation  $\langle N(t)(N(t)-1) \rangle_{\mu} \approx \langle N(t)^2 \rangle_{\mu} \approx \langle N(t) \rangle_{\mu}^2$  is often used to write from (2.10) a closed equation for the mean number of particles. This mean-field equation, obtained by replacing  $F_2$  by  $F_1^2$  in (2.9) for  $n = 1$ , predicts a  $t^{-1}$  algebraic decay of the number of particles. Clearly, the mean-field approximation will breakdown at long times when the number of particles is smaller. Many works have been devoted to describe fluctuations and deviations from mean field due to a finite number of particles [4, 7, 28]. In particular, it is possible to show that solving equation (2.9) is equivalent to computing the moments of the solution of a stochastic differential equation with a pure imaginary noise [4, 15]. However, this approach cannot be directly applied when the interaction radius is finite and transport is present. Reactions and spatial location of particles cannot be treated separately as it is usually done in reaction-diffusion systems, where the *well-mixed* hypothesis is assumed at the scale of the lattice spacing. The hierarchy of transport equations (2.7) naturally couples the spatial distribution of particles and the reactions. The aim of the next section is to provide a formal solution of (2.7) in terms of Lagrangian trajectories (or tracers) of the carrier flow. These trajectories are completely defined by carrier flow and do not depend on the reactions.

### 3 A Lagrangian approach to particle reaction kinetics

#### 3.1 Finite-number closure and recursive solutions

We now consider a finite interaction distance so that the presence of transport by the flow must be explicitly accounted for. Without loss of generality, we can assume that at  $t = 0$  the total number of particles is fixed and equal to  $N_0$ . As  $\mathcal{F}_n = 0$  for all  $n > N_0$ , the hierarchy (2.7) is closed at the order  $N_0$  and can be integrated.

Let us start with the joint  $N_0$ -point density

$$\frac{\partial \mathcal{F}_{N_0}}{\partial t} + \sum_{i=1}^{N_0} \nabla_{\mathbf{x}_i} \cdot [\mathcal{F}_{N_0} \mathbf{v}(\mathbf{x}_i, t)] = -\mu \mathcal{F}_{N_0} \sum_{i < j \leq N_0} \theta(a - |\mathbf{x}_i - \mathbf{x}_j|), \quad (3.1)$$

which can be formally solved in term of Lagrangian trajectories — that is using the method of characteristics. Denoting by  $\mathbf{Y}(t; \mathbf{y})$  the solution to the differential equation

$$\frac{d}{dt} \mathbf{Y}(t; \mathbf{y}) = \mathbf{v}(\mathbf{Y}(t; \mathbf{y}), t), \quad \mathbf{Y}(0; \mathbf{y}) = \mathbf{y}, \quad (3.2)$$

it is straightforward to check that the solution of (3.1) is given by

$$\begin{aligned} \mathcal{F}_{N_0}(\mathbf{x}_1, \dots, \mathbf{x}_{N_0}, t) &= \\ &= \int \mathcal{F}_{N_0}^0 \mathbf{e}^{-\mu \sum_{i < j \leq N_0} \int_0^t \theta(a - |\mathbf{Y}(s; \mathbf{y}_i) - \mathbf{Y}(s; \mathbf{y}_j)|) ds} \prod_{i=1}^{N_0} \delta(\mathbf{Y}(t; \mathbf{y}_i) - \mathbf{x}_i) d\mathbf{y}_1 \dots d\mathbf{y}_{N_0} \\ &\equiv \left\langle \mathcal{F}_{N_0}^0 \mathbf{e}^{-\mu \sum_{i < j \leq N_0} \int_0^t \theta(a - |\mathbf{Y}(s; \mathbf{y}_i) - \mathbf{Y}(s; \mathbf{y}_j)|) ds} \right\rangle_{N_0}, \end{aligned} \quad (3.3)$$

with  $\mathcal{F}_{N_0}^0(\mathbf{y}_1, \dots, \mathbf{y}_{N_0}) = \mathcal{F}_{N_0}(\mathbf{y}_1, \dots, \mathbf{y}_{N_0}, 0)$ . We have introduced here the so-called Lagrangian average  $\langle \cdot \rangle_{N_0}$ , which is an average over all  $N_0$ -uplets of non-reacting trajectories such that their location at time  $t$  is  $\mathbf{x}_1, \dots, \mathbf{x}_{N_0}$ . Such an average is often used in compressible transport [16]. We can now insert the expression for  $\mathcal{F}_{N_0}$  in the equation for  $\mathcal{F}_{N_0-1}$  obtaining

$$\begin{aligned} \frac{\partial \mathcal{F}_{N_0-1}}{\partial t} + \sum_{i=1}^{N_0-1} \nabla_{\mathbf{x}_i} \cdot [\mathcal{F}_{N_0-1} \mathbf{v}(\mathbf{x}_i, t)] &= -\mu \mathcal{F}_{N_0-1} \sum_{i < j}^{N_0-1} \theta(a - |\mathbf{x}_i - \mathbf{x}_j|) \\ &\quad - \mu \left\langle \mathcal{F}_{N_0}^0 \mathbf{e}^{-\Lambda_{N_0}(t)} \sum_{i=1}^{N_0-1} \theta(a - |\mathbf{Y}(t; \mathbf{y}_i) - \mathbf{Y}(t; \mathbf{y}_{N_0})|) \right\rangle_{N_0}, \end{aligned} \quad (3.4)$$

where

$$\Lambda_n(t) = \mu \sum_{i < j \leq n} \int_0^t \theta(a - |\mathbf{Y}(s; \mathbf{y}_i) - \mathbf{Y}(s; \mathbf{y}_j)|) ds. \quad (3.5)$$

The solution of Eq.(3.4) reads

$$\begin{aligned} \mathcal{F}_{N_0-1}(\mathbf{x}_1, \dots, \mathbf{x}_{N_0}, t) &= \left\langle \mathcal{F}_{N_0-1}^0 \mathbf{e}^{-\Lambda_{N_0-1}(t)} \right\rangle_{N_0-1} \\ &\quad - \mu \left\langle \mathcal{F}_{N_0}^0 \mathbf{e}^{-\Lambda_{N_0-1}(t)} \sum_{i=1}^{N_0-1} \int_0^t \theta(a - |\mathbf{Y}(s; \mathbf{y}_i) - \mathbf{Y}(s; \mathbf{y}_{N_0})|) \mathbf{e}^{\Lambda_{N_0-1}(s) - \Lambda_{N_0}(s)} ds \right\rangle_{N_0}. \end{aligned} \quad (3.6)$$

The general solution for  $\mathcal{F}_n$  can be obtained reintroducing (3.6) in (2.7) solving for  $\mathcal{F}_{N-2}$  and iterating until the order  $n$ .

In writing (3.2) we have implicitly assumed the existence and uniqueness of the Lagrangian trajectories and each trajectory is labeled by its initial position. This assumption is guaranteed as we have considered a smooth velocity field. For a fully turbulent flow and if  $a$  is much larger than the Kolmogorov length scale, the velocity field is no longer smooth but only Hölder continuous with an exponent smaller than one. In such a case the solutions to (3.2) are not unique and the deterministic Lagrangian flow breaks down. However, a statistical description of Lagrangian trajectories is still possible [16].

We conclude this subsection by noticing that this new approach in terms of Lagrangian trajectories allows us to directly apply known results from passive (non-reacting) transport (see [12] for a review) to address the problem of advection-reaction. These theoretical considerations will be mostly used in Sect. 4.

### 3.2 Long times and very dilute closures

When considering very dilute systems and small interaction radii, the hierarchy of transport equations can be closed at each order as the second term of the right hand side of Eq. (2.7) can be neglected with respect to the first one. In particular, the closure becomes exact in the long time limit when the mean number of particles depends only on the statistics of the relative distance of one pair of Lagrangian trajectories.

The long time behavior of the joint  $n$ -point density can be directly obtained from equation (3.6). Noticing that  $\Lambda_{N_0-1}(s) - \Lambda_{N_0}(s) < 0$ , at the leading order, the joint  $n$ -point density is given for  $n \geq 2$  by

$$\mathcal{F}_n(\mathbf{x}_1, \dots, \mathbf{x}_n, t) = \left\langle e^{-\Lambda_n(t)} \right\rangle_n. \quad (3.7)$$

Integrating over all spatial variables, for  $n \geq 2$ , we obtain

$$F_n(t) = \left\langle \mathcal{F}_n^0 e^{-\mu \sum_{i < j}^n \int_0^t \theta(a - |\mathbf{Y}_i(s) - \mathbf{Y}_j(s)|) ds} \right\rangle \quad (3.8)$$

where now the average is over all possible  $n$ -uplets of tracers. Finally, averaging the factorial moments over the realizations of the velocity field, we can define the effective reaction rate as

$$\gamma_n = -\lim_{t \rightarrow \infty} \frac{1}{t} \ln \frac{\overline{F_n(t)}}{\overline{F_n(0)}}. \quad (3.9)$$

Note that the average over different realizations of the carrier flow, denoted with an overline, is performed before taking the logarithm. This important point will be further discussed in Sect. 4.1.

In the zero-dimensional limit, by definition the Heaviside function inside equation (3.8) is equal to one, and thus the effective rate is simply given by  $\gamma_n = \mu n(n-1)/2$ , as confirmed by numerical data (not shown). When the system is not well-mixed at all scales, the effective rate (3.9) cannot be computed for generic



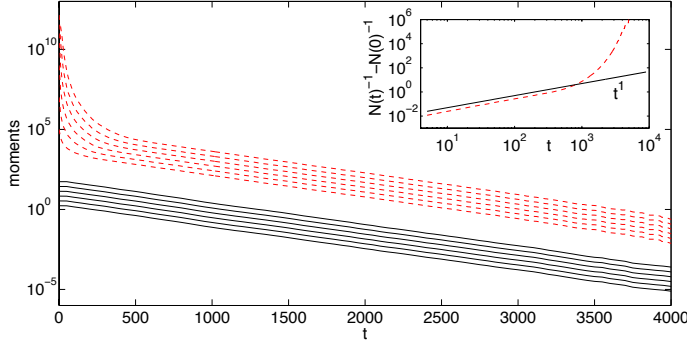


**Fig. 3.1** Temporal evolution of  $\langle N^p \rangle$  for  $p = 1, 2, 3, 4$  and initial values  $N_0 = 2$  (black solid lines) and  $N_0 = 100$  (red dashed lines). Simulations are obtained by Monte-Carlo simulations of the reactions using a delta-correlated in time velocity field (see Sec. 5 for settings of the flow). Average is taken over reactions, realizations of the flow and initial positions of particles. The parameters of the simulation are  $\mu = 1$ ,  $\varphi = 0.1$  and  $a/L = 0.015$ . The red dashed lines have been arbitrarily multiplied by a factor 1000 for the sake of representation. Inset: temporal evolution of the inverse of the average number of particles for  $N_0=100$ . It displays the mean-field prediction  $\langle N(t) \rangle_\mu \simeq N_0 / (1 + CN_0 t)$  which is indeed expected to work at short times.

flows as multi-time and space correlations of Lagrangian trajectories are involved. However, an important role is played by the case  $n = 2$  that only depends on the two-point motion. Indeed, it is easy to check from equation (3.8) that  $\gamma_n$  is an increasing function of  $n$ . In addition, the moments of the number of particles can be expressed as a linear combination of the factorial moments. The rate  $\gamma_2$  is thus always the leading exponent and for all  $p \geq 1$  we have

$$\langle N^p \rangle \sim e^{-\gamma_2 t}. \quad (3.10)$$

This exponential decrease is expected to be valid at long times regardless of the initial number  $N_0$  of particles considered. This behavior is evidenced in Fig. 3.1 where the temporal evolution of the moments  $\langle N^p \rangle$  is displayed for  $N_0 = 2, 100$  and different orders  $p$ . For  $N_0 = 100$ , the long-time departure from the  $\propto t^{-1}$  mean-field prediction is clear from the inset. Independently of the order of the moment considered, the long-time dynamics depends only on the statistics of the relative distance of one pair of tracers, which motivates the next section that is devoted to the study of the two-point motion.

## 4 Two-point motion

### 4.1 Effective rate

As the long-time behavior of the system is dominated by the two-particle dynamics, it is natural to close the hierarchy (2.7) at the second order and to look at the mean numbers of particles and of pairs:

$$n_1(t) \equiv \overline{\langle N(t) \rangle}_\mu = \overline{F_1(t)}, \quad n_2(t) \equiv \frac{1}{2} \overline{\langle N(t) [N(t) - 1] \rangle}_\mu = \frac{1}{2} \overline{F_2(t)}. \quad (4.1)$$

The overbars designate the average with respect to the realizations of the velocity field  $\mathbf{v}$ , which is assumed statistically homogeneous in space so that the overbars include the average over the particle initial positions. Both quantities,  $n_1(t)$  and  $n_2(t)$ , are expected to exponentially decrease with the same rate  $\gamma_2$ , which here and in the following will be denoted by  $\gamma$ . An effective equation describing such a behavior is simply given by

$$\frac{dn_1}{dt} = -\gamma n_2, \quad \frac{dn_2}{dt} = -\gamma n_2. \quad (4.2)$$

The effective rate  $\gamma$  depends on the microscopic rate  $\mu$ , the interaction radius  $a$  and the statistics of the carrier flow through equations (3.8) and (3.9). However, these equations do not allow us to readily obtain an explicit expression for  $\gamma$ . The dependence of such an expression on the parameters of the system can be obtained by using standard tools of dynamical system and statistical physics.

The effective rate  $\gamma$ , defined by equation (3.9), depends on the particles trajectories only through  $\mathcal{F}_2$  and thus is determined by the two-particle statistics. Consequently, without loss of generality, we will focus on a system initially having  $N_0 = 2$  particles. For such a system,  $\mathcal{F}_2^0 = 2$  and the average number of pairs reads

$$n_2(t) = \overline{e^{-\mu \int_0^t \theta(a-R(s)) ds}}, \quad (4.3)$$

where  $R(t) = |\mathbf{R}(t)| = |\mathbf{Y}_1(t) - \mathbf{Y}_2(t)|$  and the average is over all realizations of the carrier velocity field  $\mathbf{v}$ . The argument of the exponential in Eq. (4.3) contains a time integral that, for ergodic two-point dynamics, self-averages, i.e.

$$\lim_{t \rightarrow \infty} \frac{1}{t} \int_0^t \theta(a-R(s)) ds = P_2^<(a) \equiv \mathbb{P}\{R(s) < a\}, \quad (4.4)$$

where  $\mathbb{P}$  is a shorthand notation for probability. This observation leads to the following naive prediction

$$\gamma_{\text{naive}} = \mu P_2^<(a). \quad (4.5)$$

This estimate is consistent with what could be expected on a heuristic basis, however it is valid only when considering a fixed realization of the carrier flow. This kind of setting corresponds to the so-called *quenched disorder* in statistical mechanics. Indeed, let us fix a realization  $\mathbf{v}$  of the carrier flow and the initial positions  $\mathbf{X}_1(0)$  and  $\mathbf{X}_2(0)$  of the pair of reacting particles. If we now denote by  $N(t)$  the variable which is equal to 2 when the two particles have not reacted and 0 otherwise, we clearly have that

$$\lim_{t \rightarrow \infty} \frac{1}{t} \ln \langle N(t)[N(t) - 1] \rangle_\mu = - \lim_{t \rightarrow \infty} \frac{\mu}{t} \int_0^t \theta(a-R(s)) ds = -\mu P_2^<(a).$$

Notice that, here, the average is performed solely with respect to reactions. The quenched effective rate is thus given by (4.5). The average over fluid realizations can be subsequently performed but it does not modify the result (4.5) as  $\ln \langle N(t)[N(t) - 1] \rangle_\mu$  is a self-averaging quantity.

The situation is quite different when considering an *annealed disorder*, that is when the fluctuations of the carrier flow are taken into account to compute the number of pairs, according to the definition (4.3). In this case, as  $n_2$  is not a self-averaging quantity, fluctuations of the carrier flow affect the long-time behavior

and, hence,  $\gamma$  is not simply given by (4.5). In most physical situations, fluctuations of the carrier flow and randomness of the initial particle positions cannot be disregarded, so that *annealed* averages must be performed to define the effective rate (3.9). As discussed in the next subsections, in this case, the effective rate  $\gamma$  can be related to the large deviations of the fraction of time spent by two particles within a distance less than  $a$ .

#### 4.2 Large deviations of the reaction time

Determining the long-time asymptotics of  $n_2$  requires to understand the behavior of the finite-time average

$$\Theta = \frac{1}{t} \int_0^t \theta(a - R(s)) ds. \quad (4.6)$$

Under ergodicity hypotheses on the two-point dynamics, this self-averaging quantity converges at long times to  $P_2^<(a)$ . When the dynamics is sufficiently mixing, the deviations of  $\Theta$  from its average are described by a large-deviation principle [10]. The probability density function (PDF)  $p(\Theta)$  thus has the asymptotic behavior

$$-\lim_{t \rightarrow \infty} \frac{1}{t} \ln p(\Theta) = \mathcal{H}(\Theta), \quad (4.7)$$

where  $\mathcal{H}$  is a convex positive rate function, which attains its minimum, equal to zero, at  $\Theta = P_2^<(a)$ . Plugging this form in (4.3) we obtain that

$$n_2(t) \propto \int_0^\infty e^{-t(\mu\Theta + \mathcal{H}(\Theta))} d\Theta. \quad (4.8)$$

A saddle-point estimate of the integral shows that the effective rate,

$$\gamma = -\lim_{t \rightarrow \infty} \frac{1}{t} \ln n_2(t) = \inf_{\Theta \geq 0} [\mu\Theta + \mathcal{H}(\Theta)], \quad (4.9)$$

is the Legendre transform of the rate function  $\mathcal{H}$ . The convexity of  $\mathcal{H}$  implies that  $\gamma$  is a non-decreasing function of  $\mu$ .

When the reaction rate  $\mu$  is small compared to the scale of variation of  $\mathcal{H}$ , the infimum in (4.9) is attained very close to the minimum of  $\mathcal{H}$  at  $\Theta = P_2^<(a)$ . There, as a result of the central limit theorem (CLT), the rate function is approximately quadratic  $\mathcal{H}(\Theta) \simeq (\Theta - P_2^<(a))^2 / (2\sigma^2)$  and the infimum in (4.9) is attained for  $\Theta = \Theta_\star = P_2^<(a) - \mu\sigma^2$ , so that

$$\gamma \simeq \mu P_2^<(a) - \mu^2 \frac{\sigma^2}{2}, \quad (4.10)$$

where  $\sigma^2/t$  is the variance of the fraction of time  $\Theta$  spent by the pair at a distance less than  $a$ . The expression (4.10) is valid as long as  $\Theta_\star$  is close enough to  $P_2^<(a)$  to neglect the sub-leading terms in the quadratic approximation for  $\mathcal{H}$ , i.e. in the domain of validity of the CLT. Notice that (4.10) requires  $\mu \ll P_2^<(a)/\sigma^2$ . Observe also that the naive estimate (4.5) for a *quenched* velocity field only captures the linear behavior of  $\gamma$  close to  $\mu = 0$ .

The asymptotic behavior of  $\gamma$  at large values of  $\mu$  relates to that of the rate function  $\mathcal{H}$  at small values of the fraction of time  $\Theta$  spent below  $a$ , indeed, from (4.9) we have

$$\lim_{\mu \rightarrow \infty} \gamma = \lim_{\Theta \rightarrow 0} \mathcal{H}(\Theta). \quad (4.11)$$

The events leading to small  $\Theta$ 's correspond to those in which the particle-pair separation remains larger than  $a$  for a very long time. More precisely, the value of  $\mathcal{H}$  at  $\Theta = 0$  relates to the distribution of the random time  $T_{\text{hit}}$  needed by pairs that are initially far apart (e.g. at separations of the order of the system size) to approach each other at a distance less than  $a$ . We can indeed write

$$\mathbb{P}(\Theta < \varepsilon) = \mathbb{P}(\Theta < \varepsilon | T_{\text{hit}} > t) \mathbb{P}(T_{\text{hit}} > t) + \mathbb{P}(\Theta < \varepsilon | T_{\text{hit}} < t) \mathbb{P}(T_{\text{hit}} < t). \quad (4.12)$$

When  $T_{\text{hit}} > t$ , the two particles have never been at a distance less than  $a$ , which implies  $\mathbb{P}(\Theta < \varepsilon | T_{\text{hit}} > t) = 1$  for any  $\varepsilon > 0$ . Conversely, when  $T_{\text{hit}} < t$ , the fraction of time  $\Theta$  is finite and  $\mathbb{P}(\Theta < \varepsilon | T_{\text{hit}} < t) \rightarrow 0$  for  $\varepsilon \rightarrow 0$ . Hence, it follows that

$$\mathcal{H}(0) = - \lim_{t \rightarrow \infty} \frac{1}{t} \ln \mathbb{P}(T_{\text{hit}} > t). \quad (4.13)$$

Different behaviors of the effective rate are thus expected depending on the tail of the distribution of  $T_{\text{hit}}$ . For the proposed large-deviation approach to be valid, one expects  $\mathbb{P}(T_{\text{hit}} > t)$  to decrease at least as fast as an exponential. Otherwise, one would obtain  $\mathcal{H}(0) = 0$ , violating the convexity of  $\mathcal{H}$ . When  $\mathbb{P}(T_{\text{hit}} > t)$  decreases faster than an exponential,  $\mathcal{H}(0) = \infty$ , and the effective rate  $\gamma \rightarrow \infty$  for  $\mu \rightarrow \infty$ . The way it diverges cannot be obtained from the distribution of  $T_{\text{hit}}$  only, as it depends on the functional form of  $\mathcal{H}$  close to  $\Theta = 0$ . In the intermediate case, when  $\mathbb{P}(T_{\text{hit}} > t)$  decreases as an exponential,  $\mathcal{H}(0)$  is finite and the effective rate approaches a finite value  $\gamma_\infty = \mathcal{H}(0)$  when  $\mu \rightarrow \infty$ . Depending on whether  $\mu^* = -d\mathcal{H}/d\Theta|_{\Theta=0}$  is finite or not,  $\gamma$  saturates to  $\gamma_\infty$  for  $\mu > \mu^*$  or approaches it asymptotically. Note that an exponential behavior for the tail of the distribution of  $T_{\text{hit}}$  is not a particular case but is actually expected to be a quite generic circumstance. Indeed, when considering times much longer than all relevant timescales of the flow, memory loss implies that the hittings of  $a$  form a Poisson process, and the hitting time is an exponential random variable.

In the next subsection we introduce and study a phenomenological model for which the rate function can be explicitly computed.

#### 4.3 A phenomenological model for reactions in bounded chaotic flows

The essence of chaotic flows is the competition between stretching and folding. Stretching results from the fact that close trajectories separate exponentially at a rate given by the largest Lyapunov exponent  $\lambda$ . Folding, which is generally due to boundary conditions, prevents the inter-particle distance to grow indefinitely and is necessary for the system to converge to a statistical steady state. Qualitatively, the time evolution of the distance  $R$  between two particles resembles the trajectory shown in Fig. 4.1. The particle pair spends long times at a distance of the order of the size  $L$  of the domain and performs rare excursions to very small separations.

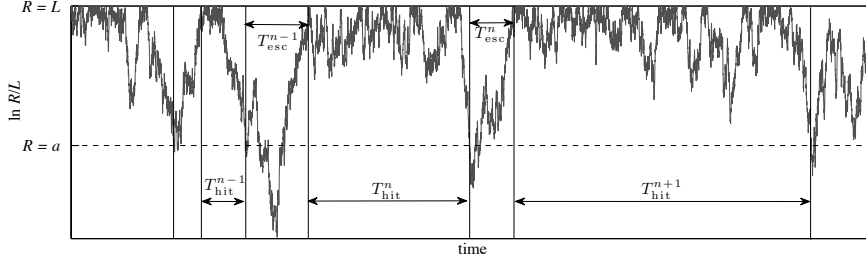


**Fig. 4.1** Illustration of the decomposition in hitting events of duration  $T_{\text{hit}}^n$  and escapes of duration  $T_{\text{esc}}^n$  as discussed in the text.

When interested in particles reacting within a distance  $a \ll L$ , it is quite natural to decompose the inter-particle dynamics in a sequence of consecutive phases, each corresponding to a given approaching event and separated by returns to  $L$ . Starting from  $R = L$ , a first time subinterval is required to hit  $a$  for the first time. Then the particle separation grows to touch again  $L$ . The time interval  $[0, t]$  is thus decomposed in  $n_{\text{rea}}$  random subintervals of length  $T_{\text{hit}}^n + T_{\text{esc}}^n$ , where  $T_{\text{hit}}^n$  is the hitting time from  $R = L$  to  $R = a$  and  $T_{\text{esc}}^n$  the time needed to reach  $L$  for the first time starting from  $a$  (see figure 4.1). Because of the memory loss occurring when the pairs are at a distance  $L$ , these sub-intervals can be considered independent and identically distributed. The first substage corresponds to many recurrences to  $R = L$  during time lengths that are independent from each other because of the imposed boundary condition. The hitting time is dominated by the sum of these recurrence times and this leads to assume that  $T_{\text{hit}}^n$  has an exponential distribution of mean  $\overline{T}_{\text{hit}}$ . Concerning the escape time  $T_{\text{esc}}^n$ , it is clear that when  $a \ll L$ , its behavior is dominated by the long-time convergence to the Lyapunov exponent. We can thus assume that it is deterministic, namely  $T_{\text{esc}}^n \approx T_{\text{esc}} = (1/\lambda) \ln(L/a)$ . In addition, in this limit, we always have  $T_{\text{esc}} \ll T_{\text{hit}}^n$  and thus

$$t \approx \sum_{n=1}^{n_{\text{rea}}} [T_{\text{hit}}^n + T_{\text{esc}}^n] \approx \sum_{n=1}^{n_{\text{rea}}} T_{\text{hit}}^n. \quad (4.14)$$

According to the discussion of the previous subsection, the times  $T_{\text{hit}}^n$  are exponentially distributed and  $n_{\text{rea}}$  is a Poisson random variable of mean  $t/\overline{T}_{\text{hit}}$ .

During the  $n$ -th interval of length  $T_{\text{esc}}^n$ , the particles spend a time  $\alpha_n T_{\text{esc}}^n$  below a distance  $a$ . The total fraction of time spent at  $R < a$  can thus be written as

$$\Theta = \frac{1}{t} \sum_{n=1}^{n_{\text{rea}}} \alpha_n T_{\text{esc}}^n \approx \frac{n_{\text{rea}}}{t} \overline{\alpha} T_{\text{esc}}, \quad (4.15)$$

where  $\overline{\alpha}$  designates the average fraction of time spent below  $a$  during  $T_{\text{esc}}$ . We have assumed in this model that the fluctuations of  $\alpha$  do not play an important role. Notice that under these assumptions,  $P_2^<(a) = \Theta = \overline{\alpha} T_{\text{esc}}/\overline{T}_{\text{hit}}$ . We see from equation (4.15) that  $\Theta$  is proportional to  $n_{\text{rea}}$ . Its probability density is thus given by the Poisson distribution. Using the Stirling formula when  $t \rightarrow \infty$ , we obtain

$$\mathcal{H}(\Theta) = \frac{1}{\overline{T}_{\text{hit}}} - \frac{\Theta}{\overline{\alpha} T_{\text{esc}}} \left( 1 + \ln \left[ \frac{\overline{\alpha} T_{\text{esc}}}{\Theta \overline{T}_{\text{hit}}} \right] \right). \quad (4.16)$$

It is easy to check that  $\mathcal{H}(\Theta)$  given by (4.16) is a convex function that vanishes at its minimum reached at  $\Theta_{\min} = \bar{\alpha} T_{\text{esc}} / \bar{T}_{\text{hit}} = P_2^<(a)$ , as expected. Also, one sees that  $\mathcal{H}(0) = 1/\bar{T}_{\text{hit}}$  and  $\mathcal{H}'(0) = -\infty$ , where the prime denotes the derivative with respect to  $\Theta$ . In the light of the considerations of the previous section, this implies that the effective reaction rate  $\gamma$  asymptotically converges to  $\gamma_\infty = 1/\bar{T}_{\text{hit}}$  when  $\mu \rightarrow \infty$ . With the explicit form (4.16) for the rate function we actually obtain

$$\gamma = \frac{1}{\bar{T}_{\text{hit}}} \left[ 1 - e^{-P_2^<(a) \bar{T}_{\text{hit}} \mu} \right]. \quad (4.17)$$

Note that this expression also reproduces the small- $\mu$  asymptotics (4.10) with  $\sigma^2 = P_2^<(a)^2 \bar{T}_{\text{hit}}$ .

The explicit form (4.17) relies on the strong simplifications of the particle dynamics that we have made (*cf.* Fig. 4.1). However, this model is particularly useful to understand how  $\gamma$  depends on the reaction radius  $a$ , the flow compressibility, and its chaoticity that will affect both  $P_2^<$  and  $\bar{T}_{\text{hit}}$ . The time  $\bar{T}_{\text{hit}} + T_{\text{esc}} \approx \bar{T}_{\text{hit}}$  can be seen as the recurrence time from  $a$  to  $a$ . Therefore, by the *Kac Recurrence Lemma* [20], it is expected that  $\bar{T}_{\text{hit}} \sim 1/P_2^<(a)$ . However, the proportionality factor depends on the Lyapunov exponent and on the compressibility. More precisely, by definition we have that

$$\bar{T}_{\text{hit}} P_2^<(a) = \bar{\alpha} T_{\text{esc}} = \frac{\bar{\alpha}}{\lambda} \ln(L/a), \quad (4.18)$$

so that in this model  $P_2^<$  and  $\bar{T}_{\text{hit}}$  can be explicitly related if  $\bar{\alpha}$  is known.

Determining  $\bar{\alpha}$  corresponds to computing the average fraction of time spent by a particle pair at separation  $R(t) < a$  during a time interval  $T_{\text{esc}}$  given that the initial is separation  $R(0) = a$ . We can estimate this quantity by approximating  $\rho(t) = \ln(R(t)/a)$  as a Brownian motion with drift  $\lambda$  and noise variance  $\Delta$  — which typically well describes the long-time dynamics of the relative separation between particles advected by smooth finite-correlation-time flows [2, 12] —, and thus computing the fraction of time spent in the negative half line,  $\rho(t) < 0$ , during a time interval  $T_{\text{esc}}$ . Exploiting known results for Brownian motion with drift — namely, the generalized arcsine law [1] (see Appendix A) — we can obtain an analytical expression for the PDF of  $\alpha$ , from which we derive that

$$\bar{\alpha} = \Phi((\lambda^2/\Delta)T_{\text{esc}}) = \Phi((\lambda/\Delta)\ln(L/a)). \quad (4.19)$$

The function  $\Phi$  cannot be easily expressed analytically but can be numerically computed with arbitrary precision. It strictly decreases from 1/2 to zero at infinity. In addition, the assumption on the relative particle dynamics implies that the separation  $R$  at time  $t$  between two particles which start at time 0 with a separation  $R_0$  is distributed according to the lognormal distribution

$$P(R, t) = \frac{1}{R} \frac{1}{\sqrt{2\pi\Delta}} \exp \left[ -\frac{[\ln(R/R_0) - \lambda t]^2}{2\Delta t} \right]. \quad (4.20)$$

In particular, equation (4.20) implies for the generalized Lyapunov exponent  $L(q) = \lim_{t \rightarrow \infty} \lim_{R_0 \rightarrow 0} (1/t) \ln \overline{(R/R_0)^q} = q\lambda + q^2\Delta/2$  [6]. For a smooth velocity field, if the dynamics is sufficiently mixing, statistically reversible and stationary, there

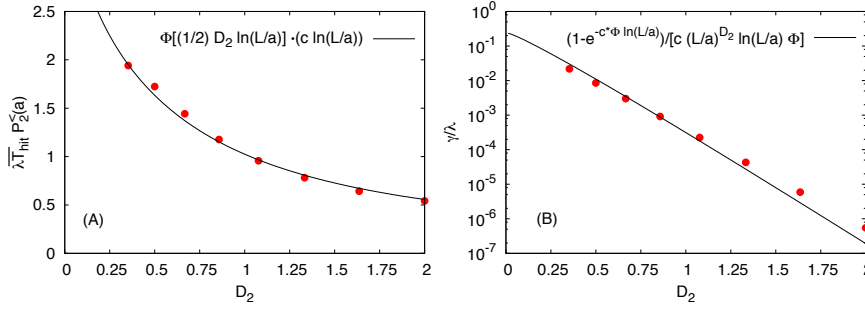


**Fig. 4.2** A) Average hitting time  $\overline{T}_{\text{hit}}$  normalized by  $1/(\lambda P_2^<)$  for  $L/a = 2000$  and as a function of  $\mathcal{D}_2$ ; the solid line correspond to the prediction (4.23) using the generalized arcsine law. B) Dependence of the effective rate  $\gamma$  (normalized by  $\lambda$ ) on the correlation dimension  $\mathcal{D}_2$  for  $\mu/\lambda = 1$  and  $L/a = 2000$ . The solid line is obtained by using equation (4.17) and  $\overline{T}_{\text{hit}}$  given by equation (4.23). In both figures the symbols show data obtained from numerical simulations using the Kraichnan flow (see section 5). The constant  $c = 1.125$  comes from the proportionality factor in equation (4.23).

is a general result stating that for a certain exponent  $\mathcal{D}_2 > 0$ ,  $(R(t)/R_0)^{-\mathcal{D}_2}$  is a conserved quantity and thus  $L(-\mathcal{D}_2)$  vanishes [18, 3]. The exponent  $\mathcal{D}_2$  coincides with the correlation dimension — a classical observable in dissipative dynamical systems (see, e.g., [23]) — that rules the scaling dependence of the stationary probability of finding two particles at a distance less than  $a$

$$P_2^<(a) \sim (a/L)^{\mathcal{D}_2} \quad \text{for } a \ll L. \quad (4.21)$$

For the lognormal distribution (4.20) we have that  $L(-2\lambda/\Delta) = 0$ , so that

$$\mathcal{D}_2 = 2\lambda/\Delta. \quad (4.22)$$

Using such a relation, the average fraction of time  $\overline{\alpha}$  (4.19) can be re-expressed in terms of  $\mathcal{D}_2$ . These considerations, together with the relation (4.18), lead us to express the average hitting time as

$$\lambda \overline{T}_{\text{hit}} \propto (L/a)^{\mathcal{D}_2} \ln(L/a) \Phi[(\mathcal{D}_2/2) \ln(L/a)]. \quad (4.23)$$

As seen in figure 4.2A, these approximations are consistent with numerical data obtained in random Gaussian compressible flows. Such flows are chosen within the Kraichnan velocity ensemble; we will come back on such numerical investigations in the next section. Note that using the above expression for  $\overline{T}_{\text{hit}}$  and equation (4.17), the effective rate  $\gamma$  normalized by the Lyapunov exponent  $\lambda$  can be expressed as function of  $\mathcal{D}_2$ ,  $a/L$  and  $\mu/\lambda$ . The dependence of  $\gamma/\lambda$  on  $\mathcal{D}_2$  is shown in figure 4.2B as a solid line and is again in good agreement with the numerical data in random flows, providing support to the approach described above. Note that there is a clear exponential decrease with  $\mathcal{D}_2$ . In general, the correlation dimension depends on the flow compressibility  $\wp$ . For incompressible flows ( $\wp = 0$ ), the trajectories are space-filling and  $\mathcal{D}_2 = d$ , the space dimension. For compressible flows,  $\mathcal{D}_2$  is a decreasing function of  $\wp$ . We thus have that, generically, compressibility enhances reactions.

The model presented in this section, although phenomenological, is based on quite general assumptions, such as the existence of a finite correlation time and of at least one positive Lyapunov exponent. The precise shape of the rate function (4.16) can vary from one system to another when more realistic dynamics is considered. It is however reasonable to expect that the general qualitative properties of the effective rate  $\gamma$  remain essentially the same.

## 5 Applications to very dilute suspensions in compressible Kraichnan flows

To illustrate and further validate the approach developed in the previous section, we focus here on two-particle motion in a special class of random velocity fields, that is the smooth (compressible) Kraichnan ensemble [16, 12]. The main advantage of such a class of stochastic flows is that, thanks to time uncorrelation, we have analytical control on most of the quantities we need. Further it is very efficient to implement numerically so to gain high quality statistics.

### 5.1 The Kraichnan velocity ensemble

We focus on dimensions  $d > 1$ . The velocity  $\mathbf{v}$  is a homogeneous, isotropic, Gaussian spatially smooth field, with zero mean and two-point correlation function

$$\overline{v_i(\mathbf{0}, t) v_j(\mathbf{r}, t')} = 2D_{ij}(\mathbf{r})\delta(t - t'), \quad D_{ij}(\mathbf{r}) = D_0\delta_{ij} - d_{ij}(\mathbf{r})/2. \quad (5.1)$$

For small separations  $r = |\mathbf{r}| \rightarrow 0$  the spatial part of the correlation is prescribed according to [16]

$$d_{ij}(\mathbf{r}) = D_1[(d + 1 - 2\wp)\delta_{ij}r^2 + 2(\wp d - 1)r_i r_j]. \quad (5.2)$$

The flow parameters are as follows: the diffusivity  $D_0$  controls the single particle dispersion properties;  $D_1$  has the dimension of an inverse time and sets the intensity of velocity gradients; finally,  $\wp \in [0 : 1]$  controls the compressibility degree as defined in Sect 2.1, its extreme values correspond to incompressible and potential velocity fields, respectively. When advecting particles with the velocity field defined by Eqs. (5.1)-(5.2), we will always consider the presence of boundary conditions, which are necessary in order to ensure statistical steady state properties (see also below the description of the numerical implementation).

Particles evolving in such flows with the dynamics Eq. (2.1) define a stochastic dynamical systems of which we know explicitly the Lyapunov exponents,  $\lambda_k = D_1[d(d - 2k + 1) - 2\wp(d + (d - 2)k)]$  ( $k = 1, \dots, d$ ), and the rate function of the stretching rates, which is quadratic (see the review [12] for a summary of the known properties of Kraichnan flows). From the latter result it is possible to prove that the lognormal distribution (4.20) for two particle separation becomes exact at sufficiently long times with  $\lambda = \lambda_1 = D_1(d - 1)(d - 4\wp)$  and  $\Delta = 2D_1(d - 1)(1 + 2\wp)$ . In particular, for the Kraichnan model, Eq. (4.22) (see discussion in Sect. 4.3) holds true with

$$\mathcal{D}_2 = \frac{d - 4\wp}{1 + 2\wp} = d - \wp \frac{2(d + 2)}{1 + 2\wp}. \quad (5.3)$$



It is worth noticing that  $\mathcal{D}_2 = d$  for  $\wp = 0$ , which simply means volume preserving dynamics in the incompressible limit, and that  $\mathcal{D}_2 = 0$  for  $\wp_c = d/4$ , which is the value of the compressibility  $\wp$  above which the first Lyapunov exponent becomes negative. The latter property indicates that above a critical compressibility  $\wp_c$  there is a transition to a regime of particles trapping with particles asymptotically collapsing onto a single point see, e.g., Ref. [16]. Notice that this regime cannot be realized for  $d > 4$ .

The intuitive content of the lognormal behavior (4.20) is that the log of the separation between the particles,  $\ln[R(t)]$ , essentially behaves as Brownian motion with drift  $\lambda$  and diffusion coefficient  $\Delta/2$ , but for the presence of boundaries at  $R = L$ . We will see in the following subsection that this is a very good approximation, which will be exploited to model the two-point quantities we are interested in, similarly to what has been done in Sect. 4.3.

In the following we will focus on the two-dimensional ( $d = 2$ ) compressible Kraichnan model, which is the simplest non-trivial example and is quite efficient for numerical implementations. In particular, we shall consider compressibility values  $\wp < \wp_c = 1/2$  to stay away from the trapping regime, which is trivial from the point of view of reaction dynamics.

As for the numerical implementation we consider two possible schemes. The first, which is useful when considering many particles (this is that used for Fig. 3.1), consists in generating a random velocity field, with periodic boundary conditions, as the sum of independent Fourier modes with  $|\mathbf{k}| \leq 2$  and amplitudes such that Eqs.(5.1)-(5.2) are satisfied at small scales. When interested in two-particle motion, we use a second scheme, which is much more efficient. It evolves directly the stochastic equation for the separation  $\mathbf{R}$  between the particles. We use a discretization by means of a standard Euler-Ito scheme that reads

$$\begin{aligned} R_i(t + dt) &= R_i(t) + \sqrt{2dt}V_i(\mathbf{R}, t) \quad \text{for } i = x, y \\ \text{with } V_x &= \sqrt{D_1(1+2\wp)}R_x\eta_x - \sqrt{D_1(3-2\wp)}R_y\eta_y \\ V_y &= \sqrt{D_1(1+2\wp)}R_y\eta_x + \sqrt{D_1(3-2\wp)}R_x\eta_y, \end{aligned}$$

which only requires to generate two independent zero-mean Gaussian random variables,  $\eta_i$ . The above equations indeed prescribe that  $\overline{V_i(\mathbf{R}, t)V_j(\mathbf{R}, t)} = d_{ij}(\mathbf{R})$ , with  $d_{ij}$  given by Eq.(5.2) for  $d = 2$ . Finally, to ensure a statistically steady dynamics, reflective boundary conditions are imposed at  $|R_i| = L/2$ . In principle, this scheme can be generalized also to more than two particles [13].

## 5.2 Numerical results

As discussed at length in the previous sections, the long-time statistics of very dilute systems is dominated by the two-particle effective reaction rate  $\gamma$ . This is confirmed by numerical simulations of the compressible Kraichnan flow: as shown in Fig. 3.1 the decay of the moments of the number of particles is indeed asymptotically dominated by  $\gamma$ . Therefore, here, we focus on the two-point dynamics in two-dimensional Kraichnan flows with the aim of illustrating numerically the heuristic picture set up in section 4.3.

Thanks to the Lagrangian formulation of the problem (see Sect. 3 and also Eq. (4.3)) we do not need to implement the reactions and it is enough to study the statistics of the fraction of time  $\Theta = (1/t) \int_0^t \theta(a - R(s)) ds$  spent below the reaction distance  $a$ . We can start with considering the average of  $\Theta$ , which is nothing but the probability  $P_2^<(a)$  to find the particle pair at separation below the reaction distance. For small  $a$ , we have that  $P_2^<(a) \propto (a/L)^{\mathcal{D}_2}$  (see Eq. 4.21) with the correlation dimension  $\mathcal{D}_2$  given by (5.3). Concerning the fluctuations of the self-averaging quantity  $\Theta$ , clearly its variance decays in time, i.e.  $\langle (\Theta - P_2^<(a))^2 \rangle = \sigma^2/t$ . Also, its probability distribution obeys at long times the large-deviation principle (4.7), i.e.  $p(\Theta) \sim \exp[-t\mathcal{H}(\Theta)]$ . As shown in figure 5.1, for small  $a$ , one observes that  $\sigma^2 \propto P_2^<(a)$ , so that the scaling behaviors of both  $P_2^<(a)$  and  $\sigma^2$  are controlled by the same quantity, namely the correlation dimension  $\mathcal{D}_2$ , as well verified by the numerics. (Notice that consistency between (4.17) and (4.10) would require  $\sigma^2 = P_2^<(a)^2 \overline{T_{\text{hit}}}$ , which is  $\propto P_2^<(a)$  as  $\overline{T_{\text{hit}}} \sim 1/P_2^<(a)$ ; this is verified in Fig. 5.3.) Moreover, figure 5.2 shows the rate function  $\mathcal{H}$  computed at different times for a flow with  $\wp = 0.1$  (different values of the compressibility provide qualitatively similar results). The collapse of the curves demonstrates the validity of the large-deviation principle. It is also worth noticing that for tiny deviations from the average the rate function is well approximated by the parabola  $(\Theta - P_2^<(a))^2/(2\sigma^2)$  associated to the central limit theorem. However, it is interesting to note that for larger deviations there is a clear departure from this behavior, and the rate function becomes asymmetric. This is consistent with the phenomenological expression (4.16).

In order to test the phenomenological picture discussed in section 4.3, we need to study the statistics of the hitting time  $T_{\text{hit}}$ , which is at the base of our reasoning. To this aim we perform a large number of numerical experiments where we set  $R(0) = L/2$  and measure the first time  $T_{\text{hit}}$  such that  $R(T_{\text{hit}}) = a$ . The distribution of such times is shown in Fig. 5.3 for  $\wp = 0.1$  and several values of  $a$ . We expect

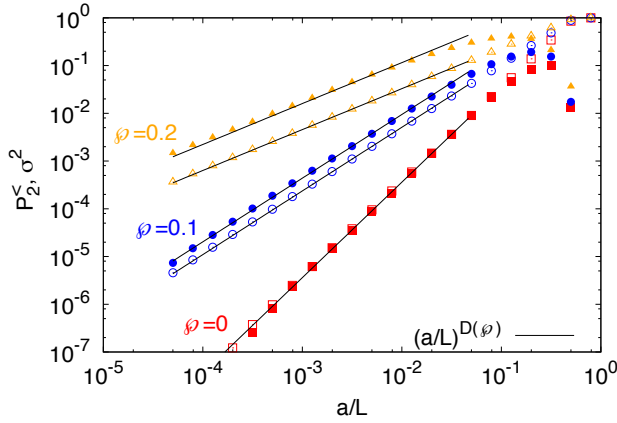


**Fig. 5.1** (Color online)  $P_2^<(a)$  (open symbols) and  $\sigma^2$  (full symbols) as a function of  $a/L$  for different compressibility values as labeled. The solid lines display the power law  $(a/L)^{\mathcal{D}_2(\wp)}$ , with  $\mathcal{D}_2(\wp)$  given by Eq. (5.3).

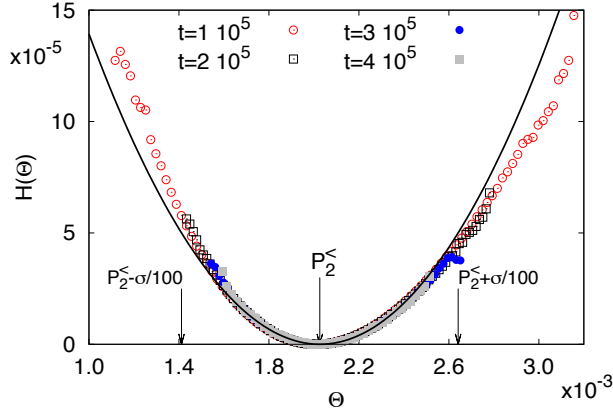


**Fig. 5.2** (Color online) The rate function  $\mathcal{H}$  as a function of  $\Theta$  for  $a/L = 5 \cdot 10^{-3}$  and  $\varphi = 0.1$  at different times as labeled. The solid black line denotes the central limit theorem approximation  $\mathcal{H}(\Theta) = (\Theta - P_2^<)^2 / (2\sigma^2)$ . The arrows show where the minimum  $\mathcal{H} = 0$  is attained, i.e. for  $\Theta = P_2^<(a)$ , and the region of validity of the approximation.

such a distribution to be exponential,  $P(T_{\text{hit}}) \approx \exp(-T_{\text{hit}}/\overline{T}_{\text{hit}})/\overline{T}_{\text{hit}}$ . As shown in the figure, this is rather well verified. Nevertheless, deviations are observed when  $a/L$  is not too small. Indeed, an exponential PDF for  $T_{\text{hit}}$  corresponds to assuming that the hitting events follow a Poisson distribution, requiring the hitting process to be memoryless. Complete memory loss can be safely assumed when  $\overline{T}_{\text{hit}} \gg 1/\lambda$  which, in virtue of (4.18), means  $\overline{T}_{\text{hit}}\lambda = \ln(L/a)/P_2^<(a) \ll 1$  so that the larger the compressibility the smaller should be  $a/L$  for the exponential PDF to be a good approximation. As shown in the inset of figure 5.3, we indeed have that  $\lambda \overline{T}_{\text{hit}} \approx 1/P_2^<(a)$ , providing a further support to (4.18) and (4.23). This is also consistent with the results shown in figure 4.2.

In principle, we can now plug the measured  $\overline{T}_{\text{hit}}$  and  $P_2^<(a)$  into equation (4.16) and compare the phenomenological prediction with the measured rate function  $\mathcal{H}$ . Although qualitatively capturing the main features of  $\mathcal{H}$ , the approximation does not really match the numerical data (not shown). Notwithstanding, the measured rate  $\gamma$  is well captured by the formula (4.17) obtained from our heuristic arguments. Clearly, this approach catches the qualitative behavior of  $\gamma$  and as seen in figure 5.4, it is also quantitatively correct both in the limit  $\mu \rightarrow 0$  where  $\gamma \approx \mu P_2^<(a)$ , and in the limit  $\mu \rightarrow \infty$  where  $\gamma \approx 1/\overline{T}_{\text{hit}}$ . In particular, figure 5.4B and its inset show how well the prediction (4.10) coming from the central-limit theorem works for small values of  $\mu$ .

In section 4.3 we have seen that approximating the evolution of  $\ln[R(t)/a]$  as a Brownian motion with drift leads to a prediction for the normalized rate  $\gamma/\lambda$  in agreement with numerical data for  $\mu = \lambda$  (Fig. 4.2). This suggests the possibility of exploiting similar ideas in order to improve the approximation for  $\gamma$  at intermediate values of  $\mu$ .

As sketched in Fig. 4.1, we decompose a time interval  $t$  in  $n_{\text{rea}}$  intervals of length  $T_{\text{hit}}^n + T_{\text{esc}}^n$ . The hitting times from  $L$  to  $a$ ,  $T_{\text{hit}}^n$ , are random, exponentially distributed variables (see Fig. 5.3). Moreover, we can assume that at time  $t$  the

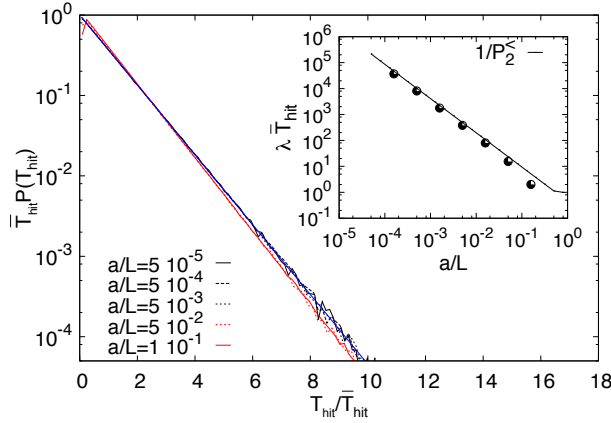


**Fig. 5.3** (Color online) PDF of the hitting time normalized with the average hitting time  $\overline{T}_{\text{hit}}$  for  $\varphi = 0.1$  for several reaction distances  $a$ , as labeled. Notice that for  $a/L \leq 5 \cdot 10^{-3}$  all curves collapse onto the exponential PDF (in blue), deviations from pure exponential PDF can be seen only for larger values of  $a/L$  (in red), which however possess a clean exponential tail. Inset: normalized average hitting time  $\lambda \overline{T}_{\text{hit}}$  vs  $a/L$  (symbols) compared to the inverse of the probability  $P_2^<(a)$ . Notice that for small-enough distances  $\overline{T}_{\text{hit}} \propto 1/P_2^<(a) \sim (a/L)^{-\mathcal{D}_2(\varphi)}$ .

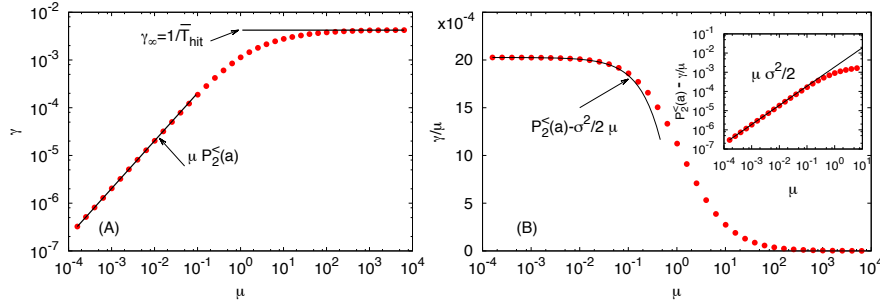


**Fig. 5.4** (A)  $\gamma$  vs  $\mu$  for  $\varphi = 0.1$  and  $a/L = 5 \cdot 10^{-3}$  the solid lines shows the small and large  $\mu$  asymptotics, respectively. (B)  $\gamma/\mu$  vs  $\mu$  the solid line displays the central-limit theorem prediction (4.10), which is made more clear in the inset by eliminating the constant term.

distribution of  $n_{\text{rea}}$  is Poissonian,  $P(n_{\text{rea}}, t) = K^{n_{\text{rea}}} \exp(-K)/n_{\text{rea}}!$ , with mean  $K = t/\overline{T}_{\text{hit}}$ . Let us denote by  $\alpha^n$  the fraction of  $T_{\text{esc}}^n$  during which the particle pair is within a distance  $a$ . We can write  $\int_0^t \theta(a - R(s)) ds = \sum_{n=0}^{n_{\text{rea}}} \alpha^n T_{\text{esc}}^n$  so that

$$\begin{aligned} e^{-\gamma} &= \overline{e^{-\mu \int_0^t \theta(a - R(s)) ds}} = \sum_{n_{\text{rea}} \geq 0} P(n_{\text{rea}}, t) \left[ \overline{e^{-\mu \sum_{n=0}^{n_{\text{rea}}} \alpha^n T_{\text{esc}}^n} \middle| n_{\text{rea}}} \right] \\ &= \sum_{n_{\text{rea}} \geq 0} P(n_{\text{rea}}, t) \left[ \overline{e^{-\mu \alpha T_{\text{esc}}}} \right]^{n_{\text{rea}}} = \sum_{n_{\text{rea}} \geq 0} P(n_{\text{rea}}, t) \beta^{n_{\text{rea}}} = e^{-(1-\beta)K} = e^{-t \frac{1-\beta}{\overline{T}_{\text{hit}}}}. \end{aligned}$$

In the above derivation we made essentially no approximation but the statistical independence of the time subintervals. This assumption is justified by the memory

loss of the process. As a result we have an explicit expression for the effective reaction rate

$$\gamma = (1 - \beta)/\overline{T_{\text{hit}}} = \gamma_{\infty}(1 - \beta), \quad (5.4)$$

which is consistent with the asymptotic behaviors for small and large  $\mu$ . Now we need to compute  $\beta$ , which can be expressed as

$$\beta = \overline{e^{-\mu\alpha T_{\text{esc}}}} = \int_0^{\infty} dT_{\text{esc}} P(T_{\text{esc}}) \int_0^1 d\alpha e^{-\mu\alpha T_{\text{esc}}} P(\alpha|T_{\text{esc}}), \quad (5.5)$$

where  $P(T_{\text{esc}})$  is the PDF of  $T_{\text{esc}}$  and  $P(\alpha|T_{\text{esc}})$  the PDF of the fraction  $\alpha$  conditioned on  $T_{\text{esc}}$ . Next, as in section 4.3, we assume  $T_{\text{esc}}$  to be non-random with  $P(T_{\text{esc}}) = \delta(T_{\text{esc}} - \lambda^{-1} \ln(L/a))$ . Also, exploiting again the approximation of the dynamics of  $\ln(R(s)/a)$  as a Brownian motion with drift, we use the generalized arcsine law [1] to express  $P(\alpha|T_{\text{esc}})$  (see Appendix A). In Fig. 5.5A, we confront in good agreement the numerically computed  $P(\alpha|T_{\text{esc}})$  and the generalized arcsine law (A.1). Finally, computing numerically the integral in equation (5.5) and using the relation (5.4) we obtain the results shown in Fig. 5.5B. The numerically computed effective rate  $\gamma$  is reasonably well described by the approximation (5.4) up to  $\mu/\lambda \lesssim 10$  (see also inset), while the approximation breaks down for larger values of  $\mu$ .

When  $\mu$  is too large, the approximation might indeed fail for two reasons. First, we should notice that  $T_{\text{esc}}$  is a random quantity defined as the first time when the separation reaches  $L$  from  $a$ . This can be taken into account by approximating  $P(T_{\text{esc}})$  in equation (5.5) with an inverse Gaussian, which also comes from considering  $\rho(t) = \ln(R(t)/a)$  as a Brownian motion with drift. However, the generalized arcsine law used to express  $P(\alpha|T_{\text{esc}})$  loses its validity when conditioning on the value of the now random  $T_{\text{esc}}$ . Second, in spite of the striking agreement in figure 5.5A, we know that the approximation of  $\rho(t)$  as a Brownian motion with drift fails at short times. For example, in the case  $\wp = 0$ , it is possible to show [2, 12] that  $d\rho/dt = \lambda \coth(2\rho) + \sqrt{\Delta} \eta(t)$ . The approximated dynamics is thus only reached when  $\coth(2\rho) \approx 1$ , that is at long-enough times.

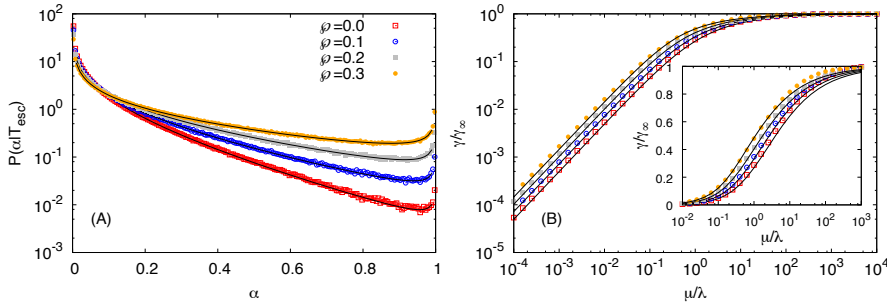


**Fig. 5.5** (A)  $P(\alpha|T_{\text{esc}})$  with  $T_{\text{esc}} = \ln(L/a)/\lambda(\wp)$  for different values of  $\wp$  as labeled and  $L/a = 2000$ . The solid lines correspond to the modified arcsine law prediction (A.1) obtained assuming a Brownian motion with drift  $\lambda(\wp) = 2D_1(1 - 2\wp)$  and diffusion coefficient  $\Delta(\wp)/2 = D_1(1 + 2\wp)$ . (B)  $\gamma/\gamma_{\infty}$  vs  $\mu$  for the same values of  $\wp$ , the solid lines correspond to (1 -  $\beta$ ), see Eq. (5.4). The inset is a zoom of the main figure in log-lin scale.

## 6 Conclusion

In this work we have considered a dilute system of particles transported by a compressible flow. The dynamics of particles was supplemented by the binary reaction  $A + A \rightarrow \emptyset$  with a rate  $\mu$ . Particles can react only when their separation is below a finite interaction radius  $a$ . We focused on a situation where transport dominates over diffusion (high Schmidt numbers) and thus particles are only driven by the carrier flow. The interest of the setting of this work is that, independently of the initial number of particles, the standard mean-field approach always breaks down at sufficiently long times. Also, due to the compressible transport, strong inhomogeneities appear in the particle spatial distribution, changing the local effective reaction rate. To describe such a system we introduced the joint  $n$ -point density that was shown to obey a hierarchy of transport equations. This hierarchy was then solved using a Lagrangian approach based on averaging over particle trajectories. The solutions are shown to decay exponentially at long times unlike the algebraic  $\propto t^{-1}$  standard mean-field prediction. Then, it was explicitly shown that all moments of the number of particles decrease with the same rate  $\gamma$ . This effective rate depends on the statistics of the relative distance between a pair of Lagrangian trajectories. One of the main results of this work was to provide a formulation of the problem in terms of non-interacting Lagrangian trajectories of the flow. This approach allowed us to apply some standard tools of statistical mechanics and passive (non-reacting) compressible transport to the problem of advection-reaction. Assuming the existence of a large deviation principle for the time that two non-reacting particles spend within a distance  $a$ , we expressed the effective rate in terms of the (Cramér) rate function. The asymptotic values of the effective rate  $\gamma$  for  $\mu \rightarrow 0$  and  $\mu \rightarrow \infty$  were obtained using general properties of the rate function. We then introduced a phenomenological model that allowed us to understand how the effective rate depends on the compressibility of the carrier flow and on the interaction radius. Finally, we numerically studied the case of reactants advected by a smooth compressible Gaussian delta-correlated-in-time flow. Numerical and theoretical results were found to be in good agreement.

Many aspects of this work can be easily extended to more complicated situations. For instance we have focused only on tracers, that is particles that just follow a prescribed flow and whose  $d$ -dimensional position space dynamics is given by equation (2.1). This choice was made in order to simplify the presentation. Most of the results presented in this work remain valid when considering particles obeying a Newton equation, that is whose dynamics is in the  $2d$ -dimensional position-velocity phase space. For instance, the expression (3.8) for the mean number of particle in terms of relative distances remains formally the same, but one has to adopt a gas kinetics approach and perform an additional integration over particle velocities. Also, we considered particles reacting within a sharp interaction radius. This hypothesis can be easily extended replacing the Heaviside function by a more general kernel, which could possibly depend on velocity differences or any other intrinsic property of the particles.

Despite these straightforward extensions, many questions are still open. For instance, we showed that factorial moments of the number of particles exponentially decrease with a rate that is an increasing function of their order. However, only in the zero-dimensional case an explicit dependence was given (namely  $\gamma_n =$

$\mu n(n-1)/2\gamma_2$ ). In  $d \geq 1$ , these effective rates depend on the joint statistics of several particle pairs. Multi-time correlations of non-independent pairs of Lagrangian trajectories directly intervene making difficult to evaluate the effective rates. Developing such theoretical tools is important not only for the reaction-advection problem but also for general questions associated with particle transport. Another issue that was not addressed in this work, corresponds to the case when the velocity flow is not smooth enough to guarantee the existence and uniqueness of the Lagrangian trajectories. This is for example, the case of turbulent flows when the interaction radius is greater than the Kolmogorov length scale. In such cases, even if the solution in terms of tracers could be in principle extended by using the statistical description of the so-called generalized Lagrangian flow [16], many of the theoretical considerations can drastically change. For instance, in these situations the relative dispersion of particles is very different from the Brownian-motion-with-drift lognormal description used in this work.

Another topic, not covered by this work, concerns events related to the right-hand side of the rate function, which corresponds to the rare situations where particles stay close for times much larger than the average. This is relevant for instance when considering the probability that particles react very fast, a situation that can lead to underestimating the amount of reactants needed in some practical applications.

Finally, a natural extension of this work is to consider more general reactions. In particular, the case of coalescence/coagulation in dilute media presents many relevant applications to different fields, such as astrophysics or geosciences. Note that an alternative approach to that given by the Lagrangian trajectories consists in trying to close the hierarchy of transport equations by performing an appropriate coarse-graining. However, because of the finiteness of the interaction radius this approach is not straightforward.

## A Generalized arcsine law

In this brief Appendix we summarize the generalized arcsine law derived in Ref.[1] for the probability density function  $P(\alpha|T)$  of the fraction of time  $\alpha$  spent in the negative semiaxis during a time interval  $T$  by a one-dimensional Brownian motion with drift  $\delta$  and diffusion coefficient  $D$ . Denoting  $Y = \delta/\sqrt{2D}$ , such a probability reads

$$P(\alpha|T) = \frac{T}{2} \left[ \left( \frac{2}{\pi T \alpha} \right)^{1/2} e^{-\frac{Y^2 T \alpha}{2}} - 2Y \chi(Y \sqrt{\alpha T}) \right] \times \quad (\text{A.1})$$

$$\left[ \left( \frac{2}{\pi T (1-\alpha)} \right)^{1/2} e^{-\frac{Y^2 T (1-\alpha)}{2}} + 2Y \left( 1 - \chi(Y \sqrt{T(1-\alpha)}) \right) \right],$$

with  $\chi(x) = \frac{1}{2} \text{erfc}(x/\sqrt{2})$ . Notice that for zero drift  $Y = 0$  the above expression recovers the standard arcsine law  $P(\alpha|T) = 1/[\pi \sqrt{\alpha(1-\alpha)}]$ .

**Acknowledgements** We acknowledge Colm Connaughton, Paolo Muratore-Ginanneschi, Marija Vucelja, Samriddhi S. Ray for many useful discussions and remarks. The research leading to these results has received funding from the European Research Council under the European Community's Seventh Framework Program (FP7/2007-2013, Grant Agreement no. 240579). MC acknowledges Observatoire de la Côte d'Azur for hospitality, and the support of MIUR PRIN-2009PYYZM5.

## References

1. Akahori, J.: Some formulae for a new type of path-dependent option. *Ann. Appl. Probab.* p. 383 (1995)
2. Balkovsky, E., Fouxon, A.: Universal long-time properties of Lagrangian statistics in the Batchelor regime and their application to the passive scalar problem. *Phys. Rev. E* **60**, 4164 (1999)
3. Bec, J., Gawędzki, K., Horvai, P.: Multifractal clustering in compressible flows. *Phys. Rev. Lett.* **92**, 224501 (2004)
4. Cardy, J.: Renormalisation group approach to reaction-diffusion problems. In: J.M. Drouffe, J.B. Zuber (eds.) *The Mathematical Beauty of Physics: A Memorial Volume for Claude Itzykson*, Saclay, France 5-7 June 1996. World Scientific, Singapore ; River Edge, NJ (1997)
5. Chertkov, M., Lebedev, V.: Boundary effects on chaotic advection-diffusion chemical reactions. *Phys. Rev. Lett.* **90**, 134501 (2003)
6. Crisanti, A., Paladin, G., Vulpiani, A.: *Products of random matrices in statistical physics*. Springer Verlag, Berlin; New York (1993)
7. Deloubrière, O., Frachebourg, L., Hilhorst, H., Kitahara, K.: Imaginary noise and parity conservation in the reaction  $A + A \rightleftharpoons 0$ . *Physica A* **308**, 135 (2002)
8. Devenish, B., Bartello, P., Brenguier, J., Collins, L., Grabowski, W., IJzermans, R., Malinowski, S., Reeks, M., Vassilicos, J., Wang, L., et al.: Droplet growth in warm turbulent clouds. *Q. J. R. Meteorol. Soc.* (2012)
9. Doi, M.: Stochastic theory of diffusion-controlled reaction. *J. Phys. A* **9**, 1479 (1976)
10. Ellis, R.: *Entropy, Large Deviations, and Statistical Mechanics*. Springer-Verlag, New-York (1985)
11. Falkovich, G., Fouxon, A., Stepanov, M.: Acceleration of rain initiation by cloud turbulence. *Nature* **419**, 151 (2002)
12. Falkovich, G., Gawędzki, K., Vergassola, M.: Particles and fields in fluid turbulence. *Rev. Mod. Phys.* **73**, 913 (2001)
13. Frisch, U., Mazzino, A., Noullez, A., Vergassola, M.: Lagrangian method for multiple correlations in passive scalar advection. *Phys. Fluids* **11**, 2178 (1999)
14. Gardiner, C., Chaturvedi, S.: The poisson representation. i. a new technique for chemical master equations. *J. Stat. Phys.* **17**, 429 (1977)
15. Gardiner, C.W.: *Handbook of Stochastic Methods for Physics, Chemistry and the Natural Sciences*. Springer-Verlag, Berlin; New York (1985)
16. Gawędzki, K., Vergassola, M.: Phase transition in the passive scalar advection. *Physica D* **138**, 63 (2000)
17. Goudon, T., Poupaud, F.: Homogenization of transport equations: weak mean field approximation. *SIAM J. on Mathematical Analysis* **36**, 856 (2004)
18. Grassberger, P., Badii, R., Politi, A.: Scaling laws for invariant measures on hyperbolic and nonhyperbolic attractors. *J. Stat. Phys.* **51**, 135 (1988)
19. Johansen, A., Oishi, J., Mac Low, M., Klahr, H., Henning, T., Youdin, A.: Rapid planetesimal formation in turbulent circumstellar disks. *Nature* **448**, 1022 (2007)
20. Kac, M.: On the notion of recurrence in discrete stochastic processes. *Bull. Amer. Math. Soc.* **53**, 10024 (1947)
21. Mattis, D., Glasser, M.: The uses of quantum field theory in diffusion-limited reactions. *Rev. Mod. Phys.* **70**, 979 (1998)
22. Maxey, M.R.: The gravitational settling of aerosol particles in homogeneous turbulence and random flow fields. *J. Fluid Mech.* **174**, 441 (1987)
23. Paladin, G., Vulpiani, A.: Anomalous scaling laws in multifractal objects. *Phys. Rep.* **156**, 147 (1987)
24. Peliti, L.: Path integral approach to birth-death processes on a lattice. *J. Physique* **46**, 1469 (1985)
25. Perlekar, P., Benzi, R., Nelson, D., Toschi, F.: Population Dynamics At High Reynolds Number. *Phys. Rev. Lett.* **105**, 144501 (2010)
26. Pruppacher, H., Klett, J.: *Microphysics of clouds and precipitation*. Kluwer Academic Publisher, Dordrecht (2010)
27. Shaw, R.: Particle-turbulence interactions in atmospheric clouds. *Ann. Rev. Fluid Mech.* **35**, 183 (2003)
28. Täuber, U.C., Howard, M., Vollmayr-Lee, B.P.: Applications of field-theoretic renormalization group methods to reaction-diffusion problems. *J. Phys. A* **38**, R79 (2005)



- 
29. Torney, C., Neufeld, Z.: Transport and aggregation of self-propelled particles in fluid flows. *Phys. Rev. Lett.* **99**, 78101 (2007)
  30. Van Kampen, N.: *Stochastic processes in physics and chemistry*. Elsevier, Amsterdam (1992)
  31. Vergassola, M., Avellaneda, M.: Scalar transport in compressible flow. *Physica D* **106**, 148 (1997)